# A novel system for quantifying the small-scale spatial variability of net radiation and its components: design and application

Georg Wohlfahrt[1]
Erich Tasser[1,2]

[1] University of Innsbruck, Austria
[2] European Academy Bolzano, Italy
www.biomet.co.at

## ABOUT

Based on the first law of thermodynamics, the energy balance states that the net radiation ($R_n$) available to the land surface is consumed in the exchange of latent (λE) and sensible (H) heat and change of heat storage within the system (S), i.e. $R_n = \lambda E + H + S$. $R_n$, in turn, depends on the net difference between short- (S) and long-wave (L) radiation entering ($_d$) and leaving ($_u$) the land surface, i.e. $R_n = S_d - S_u + L_d - L_u$.
While $R_n$ is routinely estimated on a global scale by merging several satellite data streams, the spatial scale of these satellite products is often too coarse for applications where the effects of small-scale heterogeneity in land surface properties is of interest.
In order to meet the need for $R_n$ measurements at spatial scales smaller than typical satellite pixel sizes, we present a mobile device, which allows quantifying small-scale spatial heterogeneity of $R_n$ over short-statured canopies. We first present the design of the mobile device, followed by three case studies which are meant to illustrate its potential and conclude with a discussion of its strengths and weaknesses, as well as an outlook on potential future developments.

## DESIGN

The mobile device, referred to as EcoRobot, consists of a four-component net radiometer (NR01, Hukseflux, The Netherlands) mounted on a boom, an air temperature/humidity sensor (HMP45C, Campbell Scientific, UK) in a ventilated radiation shield, a two-dimensional sonic anemometer (Windsonic, Gill, UK), a soil temperature (107, Campbell Scientific, UK) and volumetric water content (SM300, Delta-T, UK) sensor and a data logger (CR1000, Campbell Scientific, UK) and a rechargeable battery. The data logger and the battery are mounted on a backpack consisting of an aluminium frame, which also supports the radiation shield with the air temperature/humidity sensor and the sonic anemometer on a vertical extendable pole (Fig. 1).
The pole to which the net radiometer is attached features a bubble level for levelling the instrument, as well as push button for triggering measurements. The soil temperature and moisture sensors are carefully pushed into the soil down to a depth of ca. 0.05 m (Fig. 1). The data logger is programmed to scan all sensors every 5 s. Once the push button is pressed, a digital channel is short-circuited and triggers the data logger to save the current data to the memory, followed by an acoustic signal indicating a successful measurement. In addition to the four components of Rn, the data logger outputs the net radiometer body and inferred surface temperature, air and soil temperature, soil moisture, wind speed and direction.

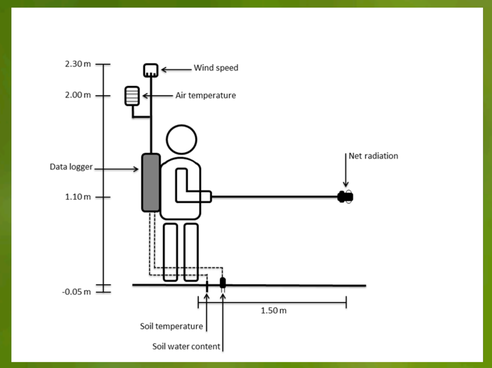


## EcoRobot design

Figure 1

Sketch of the EcoRobot design (top) and picture showing its application in the field (bottom). Indicated heights above ground in the sketch refer to an operator body size of ca. 1.8 m.

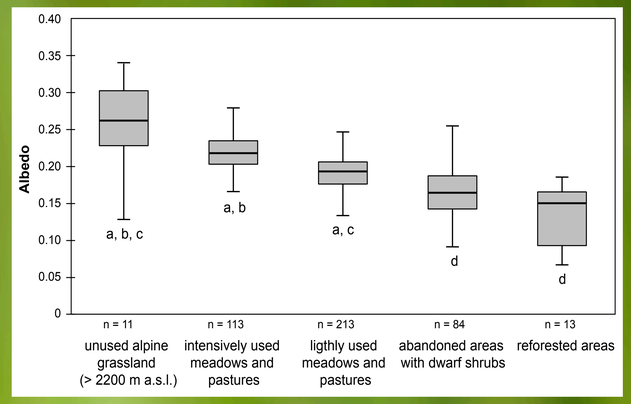


## Land-use effects on albedo

Figure 3

Relationship between land use and albedo. The boxplots show median, interquartile range and outliers. Group differences were tested with a Dunnett-T3 test ($p < 0.05$). The letters (a, b, c, d) refer to significant differences between the land-use types.

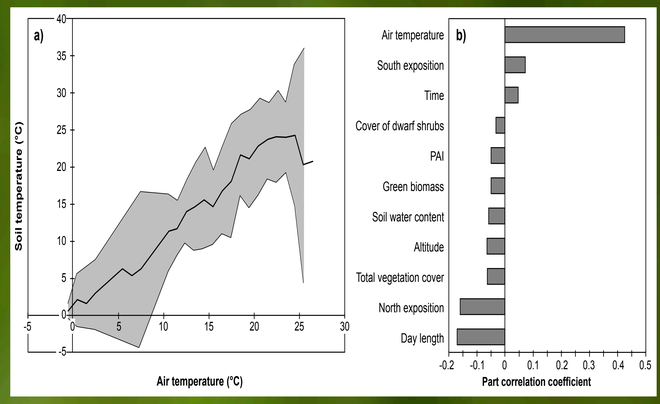


## Spatial variability in soil temperature

Figure 4

a) Comparison between air and soil temperature (solid lines with grey shading indicating 2 x standard deviation) at different grassland ecosystems. b) Result of the stepwise linear regression to model the dependence of soil temperature on explanatory variables: the Figure shows the part correlation coefficients of the significant explanatory variables.

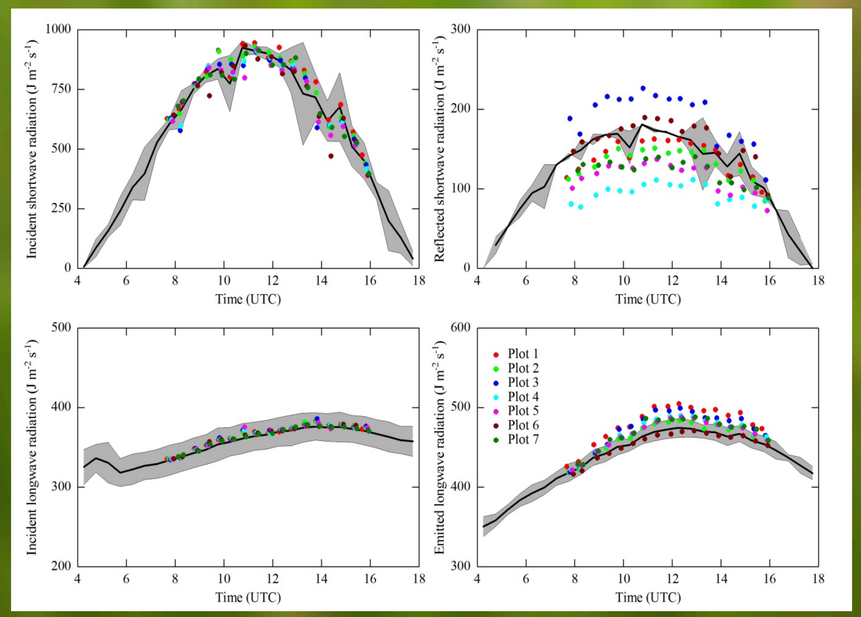


## Within-footprint variability of $R_n$

Figure 2

Comparison between stationary (solid lines with grey shading indicating 2 x standard deviation) and mobile measurements (at 7 different positions characterised by different land use within the eddy covariance flux footprint) of the four components of net radiation. The seven plots refer to the following land uses: (1) freshly seeded grassland with fraction of visible light brown dry soil, (2) densely planted butterhead lettuce, (3) butterhead lettuce covered with white fleece, (4) sparsely planted butterhead lettuce, (5) lamb's lettuce, (6) grassland similar to stationary tower surrounding, (7) grass-dominated grassland.

## CONCLUSIONS

- We have presented a mobile system for quantifying net radiation, its components and associated ancillary data (Fig. 1).
- The system operates at spatial scales (much) smaller than typical satellite pixel sizes and has great potential for quantifying the small-scale spatial variability in $R_n$ in short-statured ecosystems.
- We have demonstrated the utility of the system in two case studies: (i) For the quantification of the within-footprint spatial variability of $R_n$ at eddy covariance flux tower sites by relating stationary to mobile net radiation components (Fig. 2) – here it could be shown that the within-footprint variability in albedo and infrared surface temperature was responsible for appreciable differences as compared to the usual single-tower stationary Rn measurements. (ii) As an ecological tool for studying the small-scale variability of $R_n$ on landscape scale and the factors underlying this variability. This case study exemplified the influence of abiotic and biotic factors on soil temperature (Fig. 4) and the effect of land use on albedo (Fig. 3).
- Using the ancillary measurements (air temperature, soil temperature and moisture, wind speed) together with micrometeorological theory and some approximations related to the aerodynamic surface temperature and the soil heat flux, the mobile system in principle allows to deduce the latent heat flux as the residual of the energy balance.
- The described system could easily be up-graded with additional sensors for incoming/reflected photosynthetically active radiation, allowing the calculation of a broad-band NDVI (Wohlfahrt et al. 2010) or may be combined with portable hyper-spectral reflectance measurements (Vescovo et al. 2012).